

Supplementary Information

Contents

S1	Mathematical derivations.....	2
S1.1	Flow rate step changes.....	2
5	S1.2	Linear flow rate ramps.....3
S1.2.1	Regime A corresponding to when $t_i < 0$ and $t_f > 0$	4
S1.2.2	Regime B corresponding to when $t_i > 0$ and $t_m < t_{end}$	5
S1.2.3	Regime C corresponding to when $t_f < t_{end}$ and $t_m > t_{end}$	6
S1.2.4	Regime D corresponding to when $t_i > 0$ and $t_f > t_{end}$	7
10	S2	Flow system: Configuration 1 (ReactIR).....9
S2.1	Flow system overview.....	9
S2.2	Pumps.....	9
S2.3	Tubing and fittings.....	10
S2.4	Heating and cooling.....	10
15	S2.5	ReactIR methods.....10
S2.6	System pressure.....	12
S2.7	Residence time distribution study.....	12
S3	Flow system: Configuration 2 (on-line HPLC).....	15
S3.1	System development.....	15
20	S3.2	Configuration overview.....15
S3.3	On-line HPLC system.....	16
S3.4	On-line HPLC method for aromatic Claisen rearrangement of 6 to 7.....	16
S4	Standard transient residence time experiments.....	18
S4.1	Reverse Push Out step change (RPO step).....	18
25	S4.2	Push Out step change (PO step).....18
S4.3	Linear Reverse Push Out flow rate ramp (RPO ramp).....	19
S4.4	Linear Push Out flow rate ramp (PO ramp).....	19
S5	Solvent expansion.....	20
S6	References.....	21

S1 Mathematical derivations

S1.1 Flow rate step changes

For a generic system of reactor volume (V_R) and post reactor dead volume (V_D) before the analytical device, a step change of flow rate from an initial cumulative flow rate (Q_0) to a final cumulative flow rate (Q_{end}) performed instantaneously at $t = 0$ is evaluated as follows to determine the residence times produced:

$$V_R = \int_{t_i}^{t_f} Q(t) dt = \int_{t_i}^0 Q_0 dt + \int_0^{t_f} Q_{end} dt \quad (S1)$$

$$V_R = -Q_0 t_i + Q_{end} t_f \quad (S2)$$

There is a flow rate function discontinuity at $t = 0$ when the flow rate is instantaneously changed, leading to two integrals. Substituting for τ and rearranging gives:

$$\tau = \frac{V_R - (Q_{end} - Q_0)t_f}{Q_0} \quad (S3)$$

However the analytical device is monitoring at a fixed volume after the reactor (V_D), and so this must also be evaluated to give a function for τ in terms of the measurement time (t_m); this time only as one integral as the relevant reaction effluent in this volume will only experience the final flow rate (Q_{end}):

$$V_D = \int_{t_f}^{t_m} Q_{end} dt = Q_{end} t_m - Q_{end} t_f \quad (S4)$$

$$t_f = t_m - \frac{V_D}{Q_{end}} \quad (S5)$$

Substituting this into Equation S3 gives:

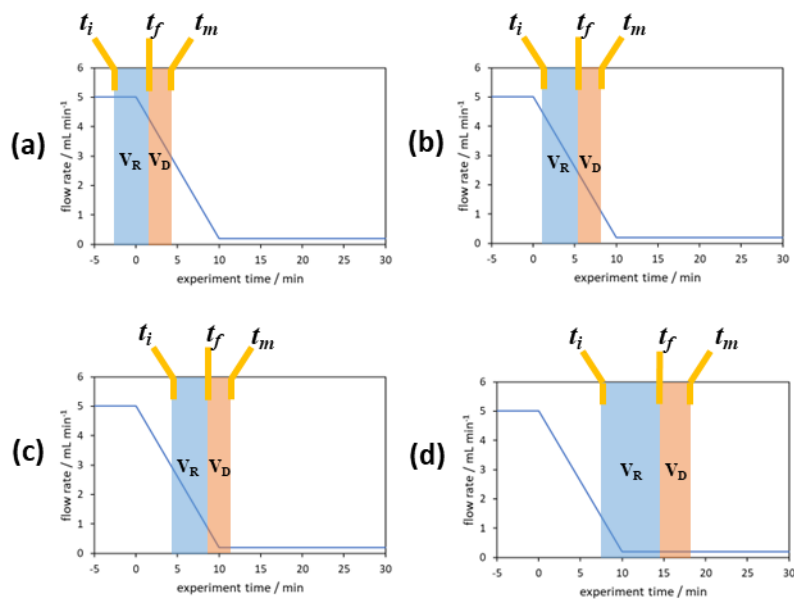
$$\tau = \frac{V_R - (Q_{end} - Q_0) \left(t_m - \frac{V_D}{Q_{end}} \right)}{Q_0} \quad (4)$$

This function for τ holds true for both PO and RPO step changes between $\tau = \frac{V_R}{Q_0}$ and $\tau = \frac{V_R}{Q_{end}}$ which when substituted into Eq. 4 give limits of t_m outside of which steady state residence times are achieved:

$$\frac{V_D}{Q_{end}} < t_m < \frac{Q_0(V_R + V_D) - Q_{end}V_D}{Q_{end}(Q_0 - Q_{end})} \quad (5)$$

S1.2 Linear flow rate ramps

For a generic system (Fig. 2) of reactor volume V_R and post reactor dead volume V_D before the analytical device, a linear flow rate ramp from an initial cumulative flow rate (Q_0) to a final cumulative flow rate (Q_{end}) at a constant ramp rate (ρ) begun at $t = 0$ and finishing at t_{end} must be evaluated in four separate regimes between the initial and final steady states (Fig. S1). In previous derivations of residence time from linear flow rate ramps, only the regime B has been evaluated and any dead volume between the end of the reactor and the analytical device (V_D , Fig. 2) was not accounted for.¹ Some work on linear residence time ramps has accounted for the dead volume, however only a single flow rate function regime was evaluated.²

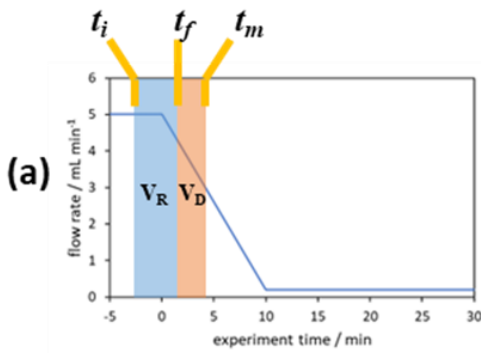


10 **Figure S1.** The graphical representation of the different regimes where the integral of the blue area corresponds to the reaction volume and that of the red area to the dead volume, in this case demonstrated on the RPO ramp from Fig. 3c.

15

20

S1.2.1 Regime A corresponding to when $t_i < 0$ and $t_f > 0$



$$t_m = 0 \quad (S6)$$

$$\tau = \frac{1}{2} \frac{\rho}{Q_0} t_f^2 + \frac{V_R}{Q_0} \quad (S7)$$

$$t_f = \frac{Q_0}{\rho} \pm \sqrt{\left(\frac{Q_0}{\rho} - t_m\right)^2 + \frac{2V_D}{\rho}} \quad (S8)$$

$$t_m = \frac{Q_0 - \sqrt{Q_0^2 - 2\rho(V_R + V_D)}}{\rho} \quad (S9)$$

This regime requires evaluation of two separate flow rate functions expressed as two limited integrals for the reactor volume:

$$V_R = \int_{t_i}^{t_f} Q(t) dt = \int_{t_i}^0 Q_0 dt + \int_0^{t_f} (Q_0 - \rho t) dt \quad (S10)$$

Integrating gives:

$$V_R = Q_0(t_f - t_i) - \frac{1}{2} \rho t_f^2 \quad (S11)$$

Substituting for τ gives:

$$\tau = \frac{1}{2} \frac{\rho}{Q_0} t_f^2 + \frac{V_R}{Q_0} \quad (S7)$$

The dead volume can be evaluated as one integral for any data after the initial steady state:

$$V_D = \int_{t_f}^{t_m} Q(t) dt = \int_{t_f}^{t_m} (Q_0 - \rho t) dt \quad (S12)$$

Integrating gives:

$$V_D = Q_0(t_m - t_f) - \frac{1}{2} \rho(t_m^2 - t_f^2) \quad (S13)$$

Solving this quadratic gives:

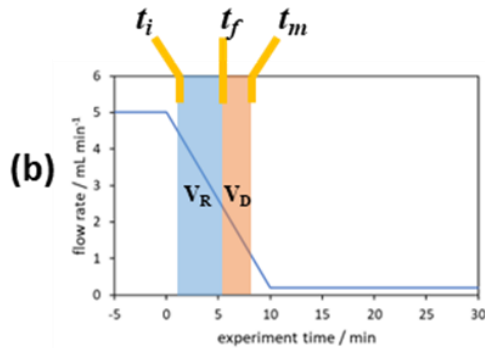
$$t_f = \frac{Q_0}{\rho} \pm \sqrt{\left(\frac{Q_0}{\rho} - t_m\right)^2 + \frac{2V_D}{\rho}} \quad (S8)$$

where the positive or negative root depends on whether a PO or RPO ramp has been performed.

The transition point between this regime and the next occurs when the reactor volume can be evaluated by one integral, transitioning when $t_i=0$, equivalent to when $t_f=\tau$. The transition point for t_m is determined by substituting Eq. S8 into Eq. S7 and rearranging to produce the limit:

$$t_m = \frac{Q_0 - \sqrt{Q_0^2 - 2\rho(V_R + V_D)}}{\rho} \quad (S9)$$

S1.2.2 Regime B corresponding to when $t_i > 0$ and $t_m < t_{end}$



$$\tau = \frac{-(Q_0 - \rho t_f) + \sqrt{(Q_0 - \rho t_f)^2 + 2\rho V_R}}{\rho} \quad (S14)$$

$$t_f = \frac{Q_0}{\rho} \pm \sqrt{\left(\frac{Q_0}{\rho} - t_m\right)^2 + \frac{2V_D}{\rho}} \quad (S8)$$

$$t_m = t_{end} \quad (S15)$$

This regime can be expressed as one integral:

$$V_R = \int_{t_i}^{t_f} Q(t) dt = \int_{t_i}^{t_f} (Q_0 - \rho t) dt \quad (S16)$$

Integrating gives:

$$V_R = Q_0(t_f - t_i) - \frac{1}{2}\rho(t_f^2 - t_i^2) \quad (S17)$$

Substituting for τ gives:

$$0 = \frac{1}{2}\rho\tau^2 + (Q_0 - \rho t_f)\tau - V_R \quad (S18)$$

Which solves to produce a solution for τ in terms of t_f :

$$\tau = \frac{-(Q_0 - \rho t_f) + \sqrt{(Q_0 - \rho t_f)^2 + 2\rho V_R}}{\rho} \quad (S14)$$

where the positive root has been taken such that when $V_R = 0$, the residence time is 0.

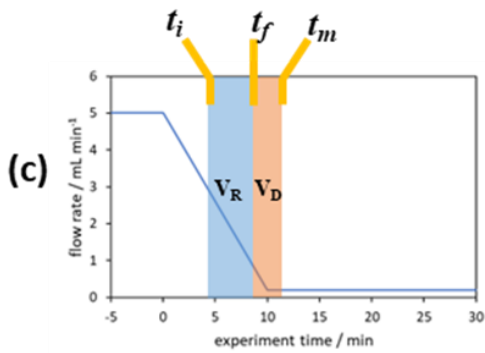
Equation S14 is similar to the equation derived by Hone *et al.*,¹ although the sign in the squared term is different, perhaps due to a typographic error. The previous derivation was used to compare between different reaction temperatures and thus replaces the reactor

volume (V_R) with the reactor length modified by a temperature dependent solvent expansion term, $\beta(T)$. For the lower temperature isothermal experiments (Knorr pyrazole synthesis and acetic anhydride hydrolysis, Scheme 1a and b), temperature dependent solvent expansion effects are negligible and can be excluded. For later studies at significantly elevated temperatures above the solvent boiling point, however, changes in solvent density have been included (Section S5). The derivation presented by Hone *et al.* does not correct for a dead volume between the end of the reactor and the analytical device (V_D). In the following derivation this has been corrected for by substituting t_f in terms of t_m as derived for regime A (Eq. S8).

The limit of this regime is when $t_m = t_{end}$ at which point the dead volume begins to fall under a two integral regime, and thus the conversion of t_f to t_m must be altered:

$$t_m = t_{end} \quad (S15)$$

S1.2.3 Regime C corresponding to when $t_f < t_{end}$ and $t_m > t_{end}$.



$$\tau = \frac{-(Q_0 - \rho t_f) + \sqrt{(Q_0 - \rho t_f)^2 + 2\rho V_R}}{\rho} \quad (S14)$$

$$t_f = \frac{Q_0}{\rho} \pm \sqrt{\left(\frac{Q_0}{\rho}\right)^2 - t_{end}^2 - \frac{2(V_D + Q_{end}t_m)}{\rho}} \quad (S19)$$

$$t_m = t_{end} + \frac{V_D}{Q_{end}} \quad (S20)$$

When the dead volume of the system is small compared to the reactor volume, regime C is likely to be unimportant as the period of time in which the dead volume need be expressed by two integrals would be short. However, in the case of a larger dead volume such a regime is important to include.

The dead volume requires evaluation of two separate flow rate functions expressed as two limited integrals:

$$V_D = \int_{t_f}^{t_m} Q(t)dt = \int_{t_{end}}^{t_m} Q_{end} dt + \int_{t_f}^{t_{end}} Q_0 - \rho t dt \quad (S21)$$

Integrating gives:

$$V_D = Q_{end}(t_m - t_{end}) + (Q_0 t_{end} - \frac{1}{2}\rho t_{end}^2) - (Q_0 t_f - \frac{1}{2}\rho t_f^2) \quad (S22)$$

And then substituting for $Q_{end} = Q_0 - \rho t_{end}$ gives:

$$V_D = Q_{end}(t_m - t_{end}) + Q_{end}t_{end} - Q_0 t_f + \rho t_f^2 \quad (S23)$$

Which solves to produce a solution for t_m in terms of t_f :

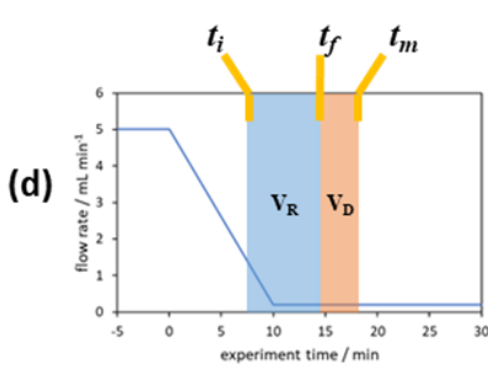
$$t_f = \frac{Q_0}{\rho} \pm \sqrt{\left(\frac{Q_0}{\rho}\right)^2 - t_{end}^2 - \frac{2(V_D + Q_{end}t_m)}{\rho}} \quad (S19)$$

where the positive or negative root depends on whether a PO or RPO ramp has been performed.

5 The limit of this regime is when $t_f = t_{end}$, obtained by rearranging equation S22 with the substitution of t_f :

$$t_m = t_{end} + \frac{V_D}{Q_{end}} \quad (S20)$$

S1.2.4 Regime D corresponding to when $t_i > 0$ and $t_f > t_{end}$.



$$\tau = \frac{-(Q_0 - \rho t_f) + \sqrt{(Q_0 - \rho t_f)^2 + 2\rho(t_{end} - t_f)(Q_0 - Q_{end}) + \rho^2(t_{end}^2 - t_f^2)}}{\rho} \quad (S24)$$

$$t_f = t_m - \frac{V_D}{Q_{end}} \quad (S25)$$

$$\tau = \frac{V_R}{Q_{end}} \quad (S26)$$

10

At the limit of regime C and D, the reactor volume integral changes from one to two limited integrals and the dead volume integral changes from two to one limited integral.

Setting the reactor volume as two limited integral:

15

$$V_R = \int_{t_i}^{t_f} Q(t) dt = \int_{t_i}^{t_{end}} (Q_0 - \rho t) dt + \int_{t_{end}}^{t_f} Q_{end} dt \quad (S27)$$

Integrating gives:

20

$$V_R = Q_0(t_{end} - t_i) - \frac{1}{2}\rho(t_{end}^2 - t_i^2) + Q_{end}(t_f - t_{end}) \quad (S28)$$

Substituting τ and rearranging to form a quadratic gives:

$$0 = \frac{1}{2}\rho\tau^2 + (Q_0 - \rho t_f)\tau - V_R + (t_f - t_{end})(Q_0 - Q_{end}) + \rho\left(\frac{t_{end}^2 - t_f^2}{2}\right) \quad (S29)$$

25

Evaluation by use of the quadratic formula, again taking the positive root, gives:

$$\tau = \frac{-(Q_0 - \rho t_f) + \sqrt{(Q_0 - \rho t_f)^2 + 2\rho(t_{end} - t_f)(Q_0 - Q_{end}) + \rho^2(t_{end}^2 - t_f^2)}}{\rho} \quad (S24)$$

When $t_m > t_{end}$, t_f can be derived as a dead volume time correction as follows:

$$V_D = \int_{t_f}^{t_m} Q(t) dt = \int_{t_f}^{t_m} Q_{end} dt = Q_{end}(t_m - t_f) \quad (S30)$$

5

Rearranging gives:

$$t_f = t_m - \frac{V_D}{Q_{end}} \quad (S25)$$

10 The final limit is dictated by the maximum residence time that can be achieved by the method.

S2 Flow system: Configuration 1 (ReactIR)

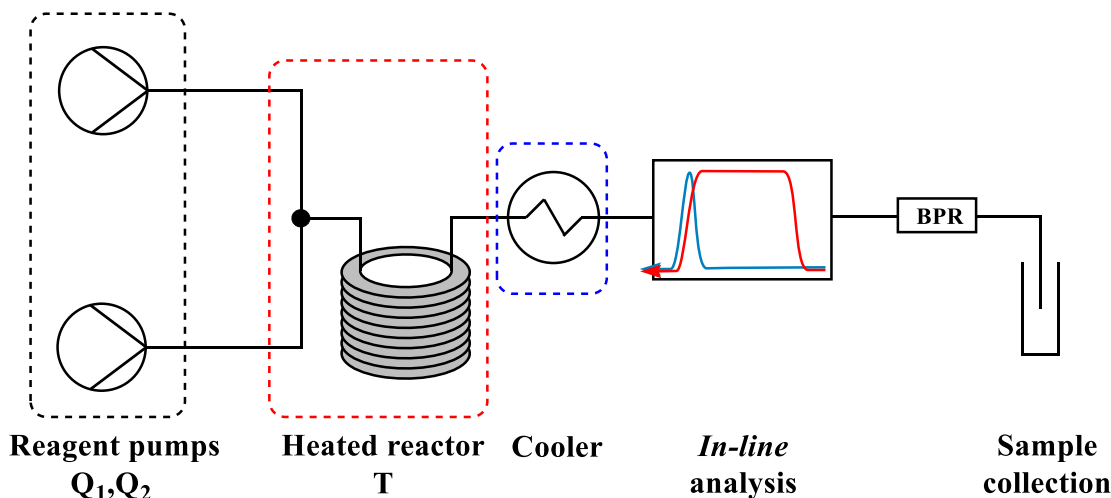


Figure S2. Schematic of the flow system for the control of individual flow rate (Q_1 and Q_2) and temperature (T), with in-line analytics.

5

S2.1 Flow system overview

A flow system (Fig. S2) was constructed, prioritising the accurate control of parameters needed for transient flow methodology to be developed. The system consisted of reactant and solvent solutions delivered from Duran bottles fitted with inlet tubing with in-line filters. The inlet tubing lines (1/8" OD, 2 mm ID PTFE, 1.6 mL and 1.2 mL respectively) were connected to two Gilson 305 HPLC pumps. The outlets of these pumps were connected to two 1 m lengths of stainless steel tubing ("SS1", 1/16" OD, 1mm ID) which fed into a Valco T-piece stainless steel mixer.

The mixer, including 0.38 m of each attached inlet line, is submerged in an oil bath, which is heated and stirred by a stirrer hotplate. The outlet of the mixer is connected to a 5.10 m tubular reactor constructed from SS1 tubing (4.13 mL internal volume), which is also submerged in the oil bath. A stainless steel HPLC style union was attached to the reactor outlet, just above the oil bath's surface, through an insulating PTFE sheet above the oil bath to a length of SS1 tubing (14 cm) which passes through a custom built cooling system consisting of an aluminium block mounted on a Peltier assembly.

The tubing is connected to the bottom fitting of the ReactIR flow cell (10 μ L) and then a 10 cm length of 1 mm ID PTFE tubing connects the outlet of the flow cell to an Upchurch Scientific 250 psi BPR set at 8.1 bar. This is connected at the outlet to a further 15 cm length of 1 mm ID PTFE tubing, which can pass into a waste container or into a vial for collection.

S2.2 Pumps

The pumps used are two Gilson 305 HPLC pumps, fitted with a 10 mL WSC and a 10 mL SC pump heads, respectively. These are connected by a GSIOC cable so that the pumps can control each other as a master/slave system through in-built Gilson firmware. In order to maintain the pumps in working order and confirm their accuracy, the check valves are cleaned and sonicated in methanol regularly, and the

cumulative flow rate of the system is confirmed at different flow rates and at different times during experimentation.

S2.3 Tubing and fittings

The pump inlet tubing is 1/8" OD, 2 mm ID PTFE tubing with a volume of 1.6 mL and 1.2 mL for pumps A and B respectively. The stainless steel tubing ('SS1') in the system is 1 mm ID, 1/16" OD from Thames Restek UK Ltd. and the T-piece is a VALCO T-piece mixer. The outlet of the back pressure regulator is connected to 1/16" OD, 1 mm ID PTFE tubing.

The fittings to the IR flow cell and connecting the BPR are 1/4-28 flat-bottom flangeless ferrules. The inlet and outlet fittings to the Gilson pumps are standard Gilson 30X fittings. All other fittings are HPLC style fittings.

10

S2.4 Heating and cooling

Heating is performed by an IKA Plate (RCT digital) stirrer hotplate with a silicon oil bath containing a magnetic stirrer bar and with a thermocouple attached for PID feedback control. Cooling is performed by a 60 W Peltier thermo-electric cooler module and heatsink assembly, procured from PiHut, with a custom cooling block milled to fit 1/16" tubing by the Advanced HackSpace, Imperial College London.

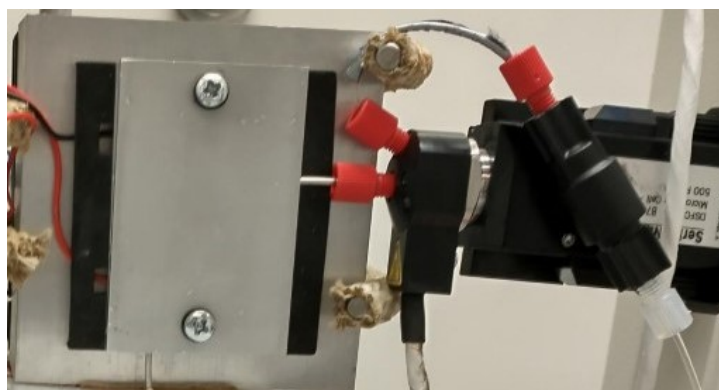


Figure S3. The cooling system used in the flow system consisting of a 60 W Peltier assembly connected to a custom aluminium block containing a cutting which fits to 1/16" stainless steel tubing. Insulation is used to cover the outside of the Peltier cooling side in order to improve the efficiency of the device by preventing direct heat transfer back across the heat junction.

20

S2.5 ReactIR methods

In-line FTIR analysis was performed utilising a Mettler Toledo ReactIR 15 instrument, equipped with a 10 μ L flow cell with a diamond ATR window. This allowed collection of reaction data at a scan rate of 15 seconds, while still affording good signal to noise.

25

Diagnostic peaks were identified for the hydrolysis of acetic anhydride from injections of acetic anhydride, acetic acid, and reaction mixtures into the IR flow cell. The optimal peaks were found in the 2nd derivative of the collected IR spectra, as the height to a two point baseline between 1004 – 992 cm^{-1} to a two point baseline at 1015 and 984 cm^{-1} (Fig. S4). Calibration of the relevant peak was performed

at the start of each experimental run by injection of stock solutions from 0.1 – 0.01 M (prepared in volumetric flasks by serial dilution) into the IR flow cell, with at least four point calibration for each experimental run. Often samples were also injected at the end of an experimental run to confirm that no drift had occurred in the selected peak. At the end of each experimental run the flow cell was flushed with ethanol and then cleaned with ethanol, water, acetone, and petroleum ethers, drying with compressed air between solvents.

5

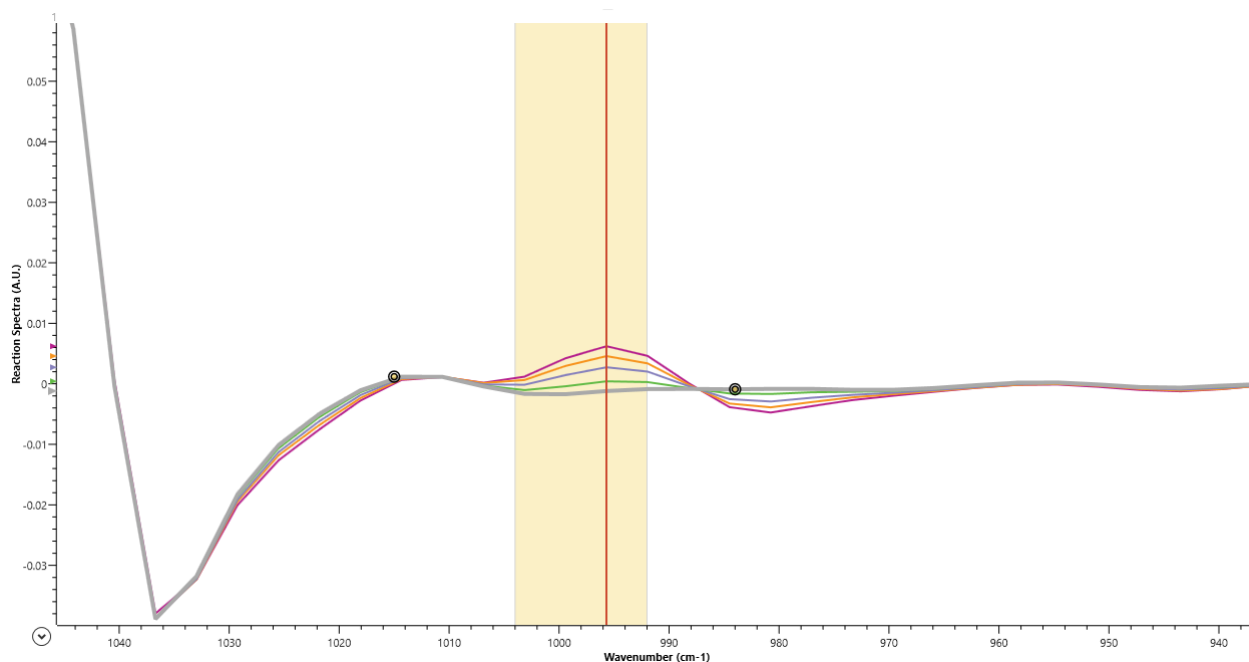


Figure S4. Example FTIR spectrum peak picking for acetic anhydride **1** on 2nd derivative processed spectra.

Diagnostic peaks were identified for the pyrazole product (**5**) corroborated by individual injections and mixed injections of the reaction
10 components, further verified by off-line HPLC. The optimal peaks were found in the 2nd derivative of the collected IR spectra as the height to a two point baseline between 1508 – 1496 cm⁻¹ to a two point baseline at 1514 and 1495 cm⁻¹ (Fig. S5). Other FTIR peaks also correlated with the pyrazole product concentration, but this peak had the best sensitivity, while remaining independent of other reaction components. Identifying unique FTIR peaks for quantification of the reactants (compounds **3** and **4**) proved challenging, and quantification was similarly
15 challenging using GC, UV/Vis, and off-line HPLC-MS, due respectively to high reactivity of starting materials, lack of distinct chromophores, and poor ionisation. Calibration was performed at the start of each experimental run by injection of known concentration samples from 0.236 – 0.028 M (prepared in volumetric flasks via serial dilution of three independent stock solutions) into the IR flow cell with at least four point calibration for each experimental run. Often samples were also injected at the end of an experimental run to confirm that no drift had occurred in the selected peak. The flow cell was cleaned in the same manner as for the hydrolysis of acetic anhydride example above.

20

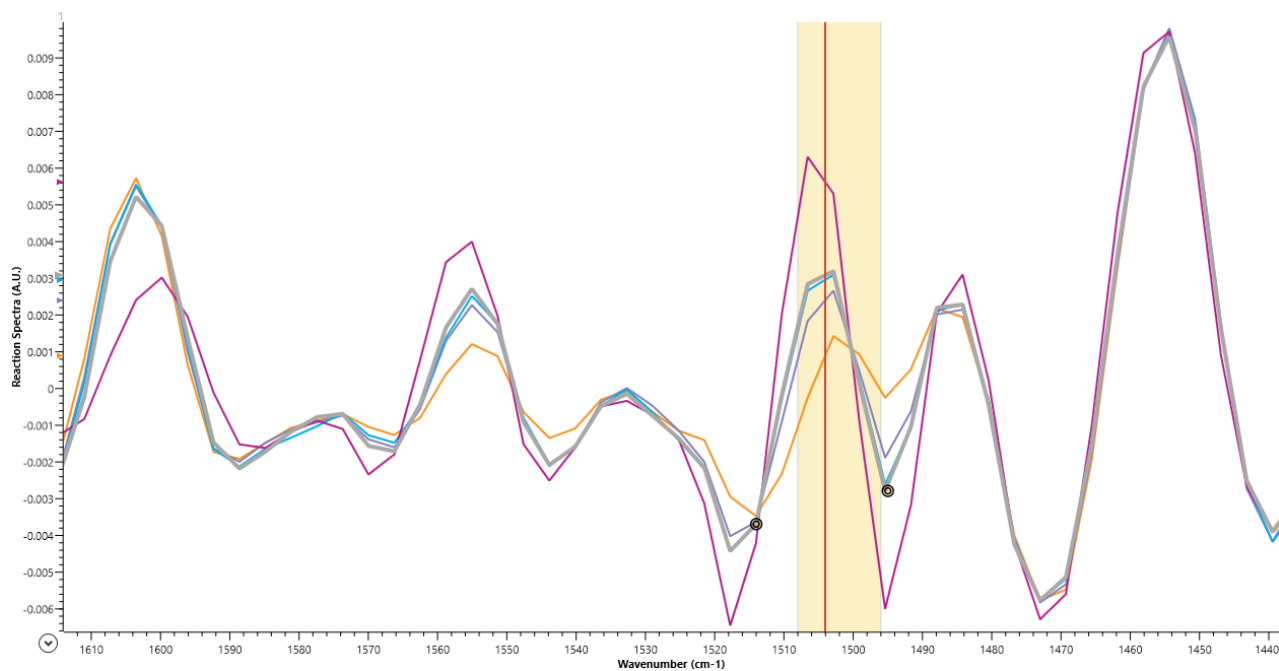


Figure S5. Example FTIR spectrum peak picking for pyrazole product **5** on 2nd derivative processed spectra.

The in-line IR spectroscopic data was collected using a Mettler Toledo ReactIR 15, equipped with a 10 μL DS Micro Flow Cell with a DComp (Diamond) probe tip. The spectrometer was set to collect spectra between 3000 cm^{-1} and 650 cm^{-1} using a resolution setting of 8 and a gain setting of 1x. A 15 second scan rate was employed in order to obtain good time resolution whilst maintain good signal to noise. Diagnostic peaks were identified for pyrazole **5** based on previous batch work and corroborated by individual injections and mixed injections of the reaction components, and by off-line HPLC. The optimal peaks were found in the 2nd derivative of the collected IR spectra as the height to a two point baseline. For **5**: between $1508\text{--}1496\text{ cm}^{-1}$ to a two point baseline at 1514 and 1495 cm^{-1} . These peaks were picked to allow maximum sensitivity for concentration of the pyrazole product whilst being independent of effects from other peaks corresponding to the reactants.

Calibration of the relevant peaks was performed at the start of each experimental run by injection of known concentration samples ranging in concentration from $0.236\text{--}0.028\text{ M}$ (prepared in volumetric flasks via serial dilution of three independent stock solutions) into the IR flow cell with at least four point calibration for each experimental run.

S2.6 System pressure

The back pressure regulator used was an Upchurch Scientific 250 psi BPR adjusted to 8.1 bar as measured for ethanol on the Vapourtec R series system. This is adequate pressure to keep all solvents used in this work in solution phase for the temperatures used.

S2.7 Residence time distribution study

Knowledge of the residence time distribution (RTD) of a flow system can allow better quality data to be produced from transient flow methods. A system with fluid dynamics similar to that of an ideal plug flow reactor (PFR), *i.e.* slow axial dispersion compared to the residence time, is the simplest to obtain reaction data from due to the assumption that each differential volume element is a self-contained

reaction.³

Utilising the pyrazole product **5** as a tracer, the RTD of the flow system was investigated by varying the flow rate ratio of a tracer solution in ethanol and a pure ethanol stream. A step change in tracer concentration was introduced to the system by maintaining a constant tracer solution pump flow rate, while performing a downwards (RPO) step change for the ethanol feed. Utilising in-line FTIR, the corresponding changes in the concentration of the tracer can be collected. Initial experiments performing step changes from ethanol with no tracer feed were hampered in curve fitting as the beginning tracer concentration changes were below the sensitivity limit of the FTIR. It was found that performing the step change in tracer concentration between two non-zero concentrations provided much more valuable data for the RTD studies. A sigmoidal change in tracer concentration was observed and was fitted to the dispersion function (Equation S32) in order to calculate the Péclet number (Pe) for this system and hence a description of the extent of the deviation of the system from an ideal PFR (Fig. S6).³

$$Pe = \frac{L u}{D} \quad (S31)$$

where Pe = Péclet number (dimensionless), L = characteristic length (m), u = local flow velocity (m s^{-1}), and D = mass diffusion coefficient ($\text{m}^2 \text{s}^{-1}$).

$$\frac{dF}{d\theta} = \frac{e^{-\frac{Pe(1-\theta)^2}{4}}}{\sqrt{\frac{12.566}{Pe}}} \quad (S32)$$

where F = normalised tracer concentration response to a step change in tracer concentration, θ = normalised residence time, and Pe = Péclet number.

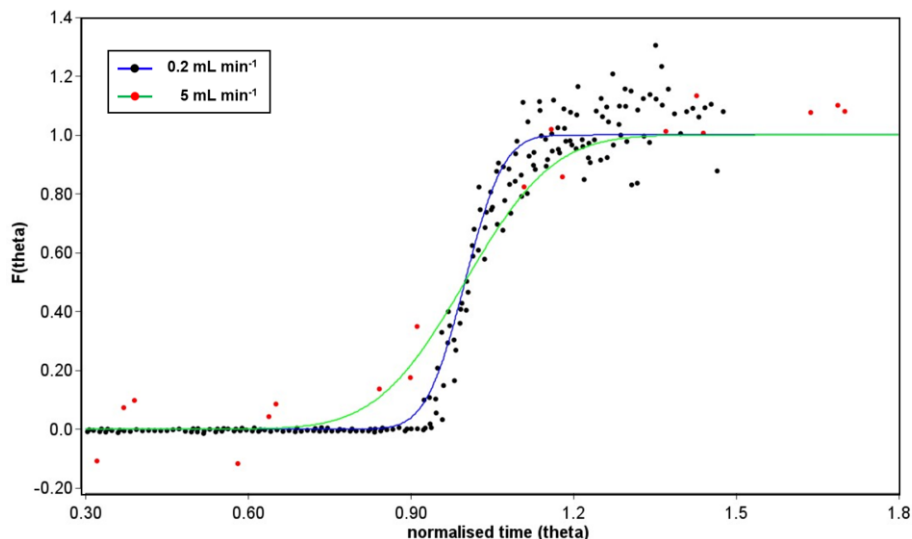
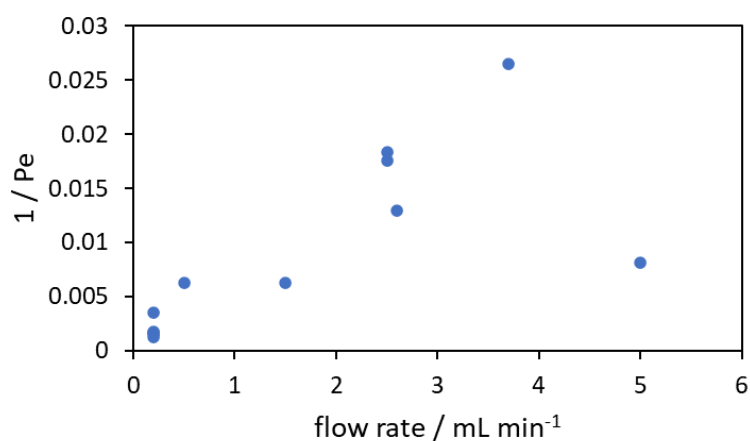


Figure S6. Example residence time distribution data fitted in Berkeley Madonna according to equation 1.2 ($F(\theta)$ vs. θ where θ = normalised residence time) to determine the Péclet number for the system under reaction conditions at the standard initial cumulative flow rate (Q_0 , 0.2 mL min^{-1}) and final cumulative flow rate (Q_{end} , 5 mL min^{-1}).

The results from the RTD study confirmed that, at the reaction temperature of $70 \text{ }^\circ\text{C}$, the mean residence times were as expected. The Péclet numbers for the flow system at minimum and maximum flow rates were calculated (at 0.2 mL min^{-1} $Pe = 690$, at 5 mL min^{-1} $Pe = 129$) and were found to have minimal deviation from an ideal PFR.

The RTD data for intermediary flow rates was then collected which suggested some intermediary flow rates produced RTD curves with a greater deviation from ideal plug flow assumptions (Fig. S7). RTD curves were collected for 0.5, 1.5, 2.5, 2.6, and 3.7 mL min⁻¹ to assess the Péclet numbers for the system. Between flow rates. 2.5 – 3.7 mL min⁻¹ dispersion coefficients ($X = 1 / Pe$) greater than 0.01 were calculated, which is the generally accepted cut off for assumption of a plug flow fluid dynamic regime. Surprisingly, this data suggests that although low (0.2 – 1.5 mL min⁻¹) and high (5 mL min⁻¹) flow rates fall under the assumption of negligible deviation from an ideal plug flow reactor, the intermediary flow rates do not. This could be explained by suggesting that high pump rates have increased pulsation which increases radial mixing, but it is also possible that the Péclet number collected at 5 mL min⁻¹ is an outlier, although the data point at 3.7 mL min⁻¹ could also. Removal of one outlier would lead to either a linear dependency of $1/Pe$ vs. flow rate, or a parabolic dependency. For the majority of the work performed in this thesis, only flow rates of 5 mL min⁻¹ or between 0.1 and 2 mL min⁻¹ were utilised, which are likely within a small deviation from ideal plug flow. Cumulative flow rate ramps utilise intermediary flow rates within this region of more complex fluid dynamics, however this appears not to affect the results.

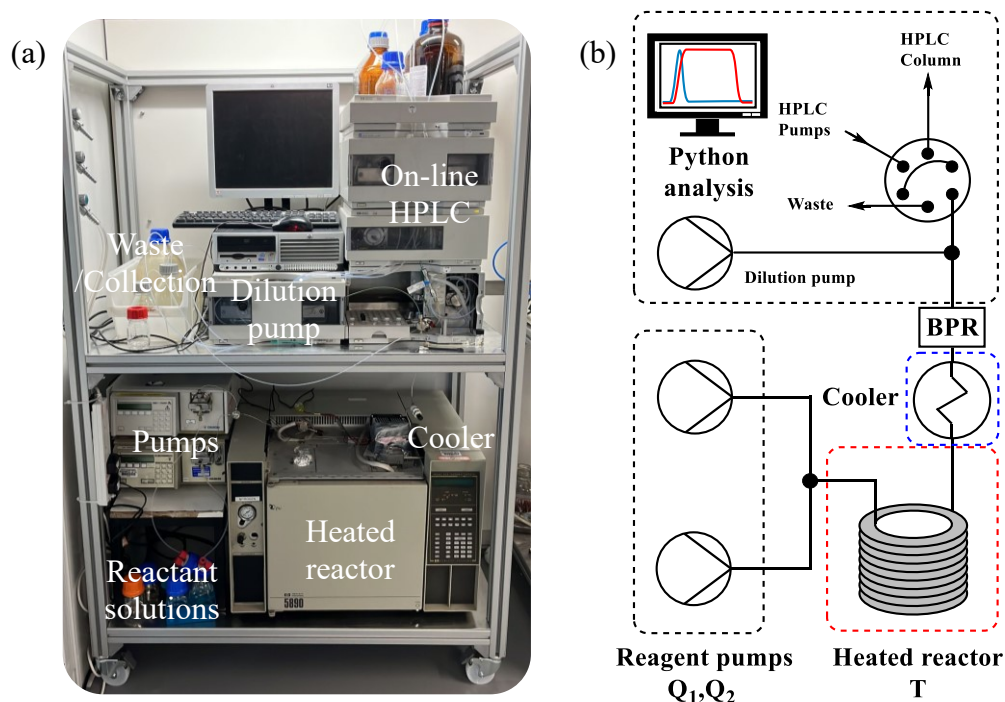


15 **Figure S7.** The quotient of the Péclet number plotted against flow rate demonstrating the changing flow regime, deviating from plug flow, with increased flow rate.

S3 Flow system: Configuration 2 (on-line HPLC)

S3.1 System development

For the study of the aromatic Claisen rearrangement (Scheme 1c), the original flow reactor system described above (S2) was modified (Fig. S8). The fluidic pathway for the reaction was generally kept the same, and therefore RTD analysis was not repeated on this system. The in-line ReactIR was substituted for an on-line HPLC system, further modified to include an in-line dilution pump for use with higher concentration reactions. The oil bath was replaced with a programmable (GC) oven, to provide accurate temperature ramping, and the back pressure regulator was changed to a one that can maintain the system under a pressure of 100 bar. The mixer was also moved out of the heated zone in order to facilitate pre-mixing of thermally activated reactions before introduction to the heated reactor.



10

Figure S8. (a) the on-line HPLC flow system constructed (configuration 2); (b) a schematic representation of the fluidic path and key components of the on-line HPLC flow system.

S3.2 Configuration overview

15 This flow system is a modification of configuration 1, as such the following description focuses on the modifications made from configuration 1 and is not meant as a comprehensive description of the flow system.

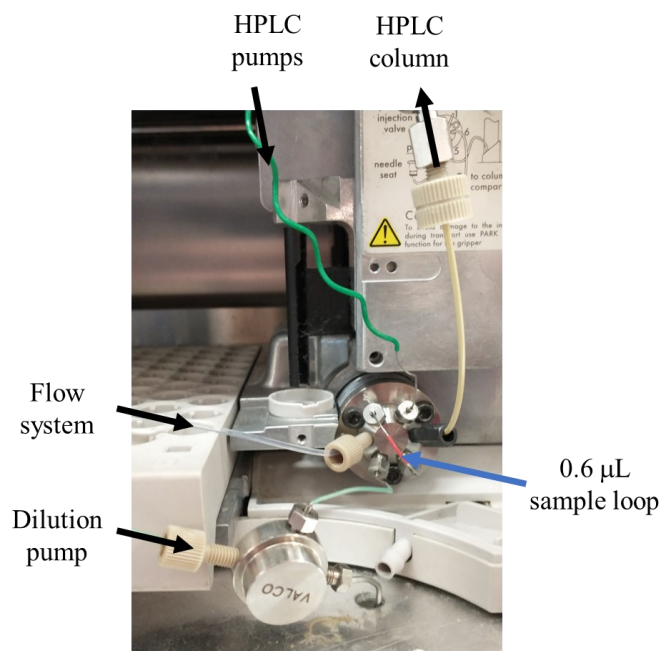
Configuration 2 flow system (Fig. S8) was constructed in which reagent(s) and solvent(s) as solutions are delivered from Duran bottles fitted with inlet tubing with in-line filters. The inlet tubing lines (1/8" OD, 2 mm ID PTFE, 1.6 mL and 1.2 mL respectively) were connected
20 to a Gilson 305 HPLC pump (pump A) and a Gilson 307 HPLC pump (pump B) respectively. The outlets of these pumps were connected to two stainless steel tubing (25 cm) which fed into a Valco T-piece stainless steel mixer.

The outlet of the mixer is connected to a 5.14 m length of stainless steel tubing ('SS1', 1 mm ID, 1/16" OD); the first 30 cm of which are outside of the GC oven (heated reactor length: 4.84 m, heated reactor volume: 3.92 mL). This is then connected by a stainless steel HPLC style union at the outlet of the GC oven through an insulating PTFE sheet to a length of SS1 tubing (14 cm) which passes through a custom built cooling system consisting of an aluminium block and a Peltier assembly. The outlet of the cooling device is connected by a stainless steel HPLC style union to a 20 cm length of SS1 tubing into a VALCO variable pressure Back Pressure Regulator (BPR). The BPR outlet is connected to a 25 cm length of stainless steel tubing which connects to a VALCO T-piece stainless steel mixer. The other mixer fittings are connected to the inlet to the modified HPLC 6-port, 2-way injector valve and to the dilution pump of the HPLC setup.

Heating of the reactor is achieved by repurposing an HP 5890 Series II GC oven, using the inbuilt software/PID to allow accurate control over temperature ramping. Cooling is performed by a 60 W Peltier thermo-electric cooler module and heatsink assembly (PiHut) with a custom cooling block milled to fit 1/16" tubing by the Advanced HackSpace, Imperial College London.

S3.3 On-line HPLC system

On-line analysis was implemented by modifying the injector on an Agilent HP 1100 series HPLC fitted with a diode array detector (DAD). The fittings to the 6-port, 2-way injector valve were disconnected and reconnected to allow a 0.6 μ L sample loop to be continually filled from the reactor effluent in the resting valve position (Fig. S9). When triggered by the Chemstation HPLC software the injector method switches the valve to its second position for 0.1 min, allowing the contents of the sample loop to be redirected by solvent from the Agilent HP 1100 series pumps into the column and subsequent detector.



20 **Figure S9.** The modified HPLC injection valve on the Agilent 1100 series G1313A autosampler for on-line HPLC analysis.

S3.4 On-line HPLC method for aromatic Claisen rearrangement of 6 to 7

The HPLC column used was a Restek Raptor C18 (2.7 μ m 50 mm x 2.1 mm) running an isocratic mixture of 40% acetonitrile in water. This method allowed injections every 4 minutes.

Table S1. Key parameters set for the HPLC method used in this example for on-line HPLC analysis.

Flow rate / mL min⁻¹	0.7
Stoptime / min	3.70
Posttime / min	0.29
Solvent A	H ₂ O
Solvent B	MeCN
DAD wavelength / nm	210

The Agilent 1100 Autosampler automatically switches the valve at the beginning of the injector program. The inputted injector cycle is a “WAIT” command for 0.10 min and then a “VALVE MAINPASS” command.

5

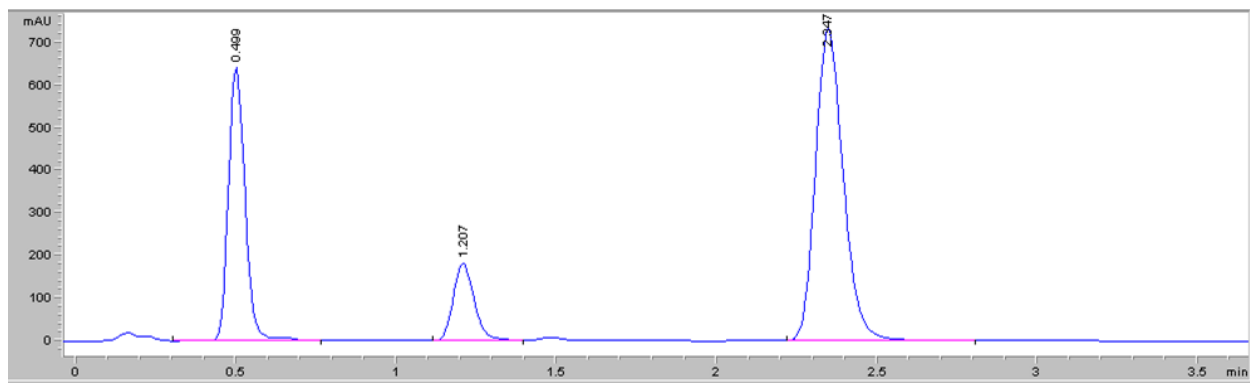


Figure S10. an example chromatogram obtained according to the HPLC method above for monitoring the reaction of *para*-methoxyphenyl allyl ether (**6**).

10 **Table S2.** Substituents for *para*-methoxyphenyl allyl ether substrates and their corresponding retention times in the HPLC method in Figure S10.

compound	Retention time / min
6	1.21
7	0.49
ethyl benzene	2.34

These data were concatenated by a python script which was developed. This script can be found at <https://github.com/LindenSchrecker>.

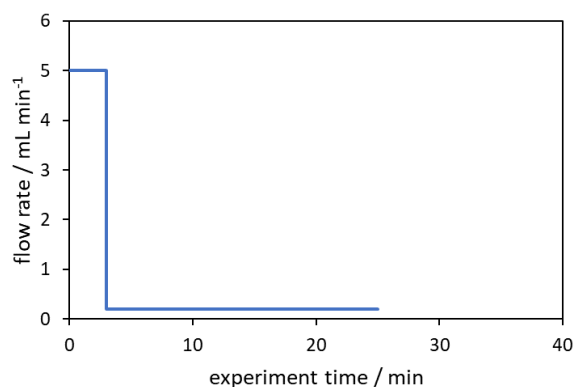
S4 Standard transient residence time experiments

S4.1 Reverse Push Out step change (RPO step)

A standard RPO step is performed by programming the pumps to begin at 5 mL min⁻¹ at a given %B ratio (flow rate ratio of pumps 1 and 2) for 3 minutes at which time the cumulative flow rate changes to 0.2 mL min⁻¹ for a further 21 minutes. This can be directly linked to other transient flow rate experiments. Once all experiments in an experimental run are finished, the system is flushed with ethanol through both pumps for at least 10 reactor volumes.

Table S3. Pump flow rate method utilised for a standard RPO step change.

time / min	flow rate / mL min ⁻¹
0	5
2.99	5
3	0.2
24.99	0.2



10 Figure S11. Cumulative volumetric flow rate method for a standard RPO step experiment.

S4.2 Push Out step change (PO step)

A standard PO step is performed by programming the pumps to begin at 0.2 mL min⁻¹ at a given %B ratio (flow rate ratio of pumps 1 and 2) for 22 minutes at which time the cumulative flow rate changes to 5 mL min⁻¹ for a further 5 minutes.

15 Table S4. Pump flow rate method utilised for a standard PO step change.

time / min	flow rate / mL min ⁻¹
0	0.2
21.99	0.2
22	5
25	5

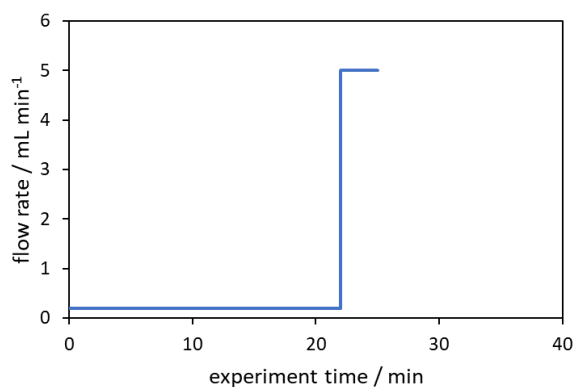


Figure S12. Cumulative volumetric flow rate method for a standard PO step experiment.

S4.3 Linear Reverse Push Out flow rate ramp (RPO ramp)

A standard RPO ramp is performed by programming the pumps to begin at 5 mL min⁻¹ at a given %B ratio (flow rate ratio of pumps 1 and 2) for 3 minutes before ramping the flow rate linearly over 10 minutes to 0.2 mL min⁻¹ which was then maintained for a further 22 minutes.

Table S5. Pump flow rate method utilised for a standard RPO ramp.

time / min	flow rate / mL min ⁻¹
0	5
3	5
13	0.2
35	0.2

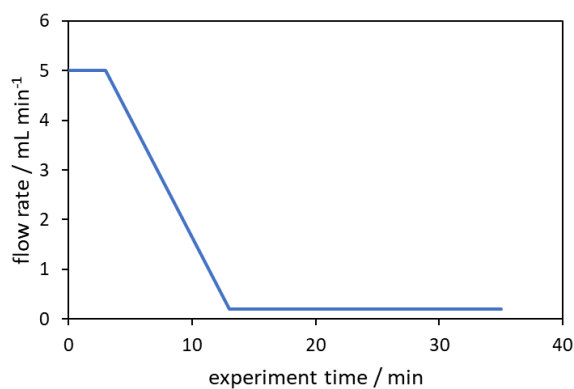


Figure S13. Cumulative volumetric flow rate method for a standard transient RPO ramp experiment.

S4.4 Linear Push Out flow rate ramp (PO ramp)

A standard PO ramp is performed by programming the pumps to begin at 0.2 mL min⁻¹ at a given %B ratio (flow rate ratio of pumps 1 and 2) for 22 minutes before ramping the flow rate linearly over 10 minutes to 5 mL min⁻¹ which was then maintained for a further 3 minutes.

Table S6. Pump flow rate method utilised for a standard PO ramp.

time / min	flow rate / mL min ⁻¹
0	0.2
22	0.2
32	5
35	5

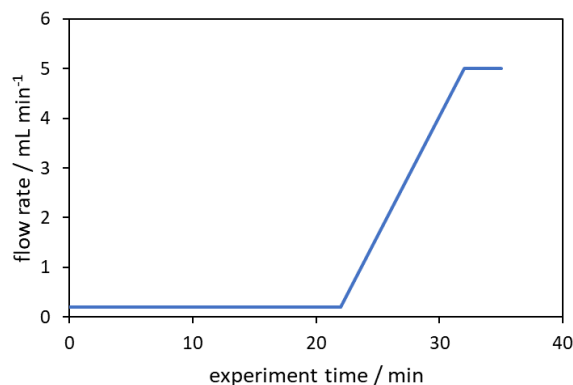


Figure S14. Cumulative volumetric flow rate method for a standard PO ramp experiment.

S5 Solvent expansion

Liquids are known to change density with changing temperature and pressure, often described simply by the Tait equations (Eq. S33 and S34 respectively).⁴ Often this effect is negligible at near-ambient conditions, but under temperatures and pressures accessible in a flow reactor the effects become more significant, leading to a variation in solvent volume and thus residence time. The Claisen aromatic rearrangement was studied at very high temperature (220 °C) and pressure (100 bar), whereupon solvent expansion becomes non-negligible.

As mentioned in S1.2.2 in discussion of Equation S14, Hone *et al.* included solvent expansion in their calculation of residence time from a transient flow rate ramp by replacing the reactor volume constant with a temperature dependent term. In this work, a different method was used to account for the solvent expansion by calculating the expected residence time if the solvent did not change density (constant reactor volume) and then modifying this term utilising the Tait equations to determine the ratio of densities under relevant conditions.⁴

This allowed true residence times to be accurately tracked allowing concentration plots to be linearised (due to first order kinetic behaviour) for error analysis of methods, as well as visual comparison of yield plots.

$$\rho_1 = \frac{\rho_0}{1 - \frac{P_1 - P_0}{E}} \quad (S33)$$

$$\rho_1 = \frac{\rho_0}{1 + \beta(T_1 - T_2)} \quad (S34)$$

where ρ = density of ethanol (kg m⁻³), P = applied pressure (bar), T = temperature (K), E = bulk modulus of elasticity (10600 bar for ethanol), and β = volumetric expansion coefficient (0.0011 K⁻¹ for ethanol).

S6 References

- 1 C. A. Hone, N. Holmes, G. R. Akien, R. A. Bourne and F. L. Muller, *React. Chem. Eng.*, 2017, **2**, 103–108.
- 2 J. S. Moore and K. F. Jensen, *Angew. Chemie Int. Ed.*, 2014, **53**, 470–473.
- 3 O. Levenspiel, *Chemical Reaction Engineering, 3rd Edition*, 1998.
- 5 4 J. H. Dymond and R. Malhotra, *Int. J. Thermophys.*, 1988, **9**, 941–951.